

## Load-follow Simulation of a 540MWth Soluble-Boron-Free SMR using CSBA

Yunseok Jeong<sup>a</sup>, Steven Wijaya<sup>a</sup>, Yonghee Kim<sup>a\*</sup>

<sup>a</sup>KAIST, 291 Daehak-ro, Yuseong-gu, Daejeon, Republic of Korea (34141)

\*Corresponding author: yongheekim@kaist.ac.kr

### 1. Introduction

Water-cooled Small Modular Reactors (SMRs) have been conceptualized to utilize soluble boron to maintain the power distribution integrity. However, relying on soluble boron may compromise reactor safety, primarily due to the near-zero Moderator Temperature Coefficient (MTC) at high soluble boron concentrations. Additionally, the limitations of boron control hinder rapid power adjustments, and integrating a complex chemical and volume control system significantly increases the overall cost of nuclear power plants.

According to the European Utilities Requirements, modern nuclear power plants are expected to seamlessly handle daily load-following operations, enabling electric output fluctuations of 3-5% of rated power per minute. As such, the importance of Soluble-Boron-Free (SBF) SMRs increases due to their improved power maneuverability [1].

Numerous designs of soluble-boron-free SMRs have been introduced to address the drawbacks associated with boron-based configurations. However, numerous alternatives have struggled to compete with commercial pressurized water reactors (PWRs) and other SMR variants. This challenge often arises from the use of conventional burnable absorber designs and the complexities of establishing a sufficient shutdown margin for cold shutdown within the constraints of a limited number of control element assemblies (CEAs). In this context, the ATOM core design, an advanced soluble-boron-free concept, emerges as a promising solution. Notably, the ATOM design effectively addresses prevailing issues related to cold shutdown margin and complexities in burnable absorber [2,3].

The investigation aims to assess the load-following capability of an enhanced soluble-boron-free ATOM core. This core configuration features an increased power output of 540MWth with an active core height of 240cm, as compared to its predecessor. The response of the core is thoroughly evaluated using the Mode-Y control logic for CEAs. To perform these simulations, the study utilizes the features of KAIST Advanced Nuclear Tachygraphy (KANT), an in-house time-dependent thermal-hydraulics coupled nodal code [4]. The homogenized group constants are generated by using Serpent 2 code for two-step analysis.

### 2. Core Design

In this section design details to model the soluble-boron-free reactor using Centrally Shielded Burnable Absorber (CSBA) are described. The details include general design specification, CSBA loading pattern, axial enrichment and zoning pattern, and control rod specifications.

#### 2.1 General Design Specification

Operating at a thermal power of 540 MW and featuring an active core height of 240 cm, the core comprises of 69 Fuel Assemblies (FAs) utilizing a two-batch fuel management while SS-304 is utilized for the radial reflector. Notable, with the exception of the central fuel assembly (3 w/o U-235), which is discharge during each cycle. The conventional 17 x 17 fuel lattice type featuring 24 guide tubes and 1 instrumental tube is utilized. However, it deviates from the conventional design by utilizing a smaller fuel pellet radius for optimal moderator proportioning. With the presence of soluble boron, the fuel lattice is under-moderated as zero or positive moderator temperature coefficient can be obtained when the core power increases. However, in SBF conditions, the fuel lattice moderation can be enhanced by using a smaller-radius fuel pellets without any concern of soluble boron related accidents. This innovative design, named Truly-Optimized PWR (TOP), enlarges the pitch-to-diameter ratio of the fuel lattice to 1.4 or reduces the fuel pellet radius to 0.38 cm while fixing the pin pitch. In this study, the smaller fuel radius TOP is implemented. Implementing TOP design in SBF PWR cores has demonstrated several benefits, including improved neutron economy and shutdown margin [3]. The detailed reactor parameters are described in Table 1.

Table 1. Specification of the core

Parameters	Value
Thermal power	540 MWth
Fuel Shuffling	Two-batch
Number of fresh FA	35
Fuel materials, enrichment	UO <sub>2</sub> , 4.95 w/o
Radial reflectors	SS-304
Axial active core height	240 cm
BA design	CSBA
BA material	Monoclinic Gd <sub>2</sub> O <sub>3</sub>
Gd <sub>2</sub> O <sub>3</sub> theoretical density	8.33 g/cc
Gd <sub>2</sub> O <sub>3</sub> density	7.40 g/cc (89% TD)
FA type, total number of FA	17 x 17, 69
Fuel pellet radius	0.38 cm

Reactivity swing (target)	1,000 pcm
Pin pitch (cm)	1.26 cm
Inlet & Outlet coolant Tem.	295.7/323 <sup>0</sup> C

## 2.2 CSBA Loading Pattern

Two cylindrical CSBAs are located within the fuel pellets with 89% theoretical density of monoclinic Gd<sub>2</sub>O<sub>3</sub>. In addition, the fuel pins close to guide thimbles contain 0.8% Er<sub>2</sub>O<sub>3</sub> to decrease the pin power peaking factor throughout cycles with negligible reactivity penalty. To achieve a flat power distribution various types of CSBA are utilized in the core. While the volume and height-to-diameter (H/D) of CSBA are adjusted to control the spatial self-shielding of CSBA at each zone. A visual sketch and specific values for the adjustments are provided in Figure 1 and Table 2.

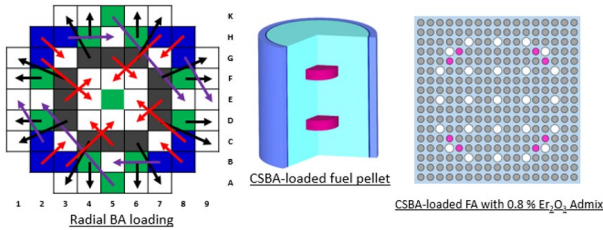


Figure 1. Radial CSBA zone and batch (1), pellet sketch (2), lattice design (3)

Table 2. CSBA volume and H/D parameters

Parameters	Optimal CSBA loading			
	Zone I	Zone II	Zone III	Control FA
CSBA design	2-Cylinder	2-Cylinder	2-Cylinder	2-Cylinder
Cylinder diameter	3.19 mm	2.66 mm	2.42 mm	2.66 mm
Cylinder height	0.98 mm	0.88 mm	0.80 mm	0.88 mm
H/D ratio	0.31	0.33	0.33	0.33
Gd <sub>2</sub> O <sub>3</sub> density (0.89% TD)	7.400 g/cc	7.400 g/cc	7.400 g/cc	7.400 g/cc

## 2.3 Axial Enrichment and Blanket

In this study, an alternative approach is adopted by employing the axial zoning of fuel enrichment instead of axial CSBA volume zoning. This approach serves to counterbalance the skewness in axial power distribution arising from the distinct axial MTC, given the coupled thermal-hydraulic calculation condition. In contrast to the previous 200 cm core, the utilization of a simple axial zoning enrichment is more practical than axial CSBA zoning.

In this configuration, the lower half of the core comprises of less fuel enrichment of 4.79 w/o. In addition, blankets consisting of 3 w/o were placed at the top and bottom with a thickness of 5 cm.

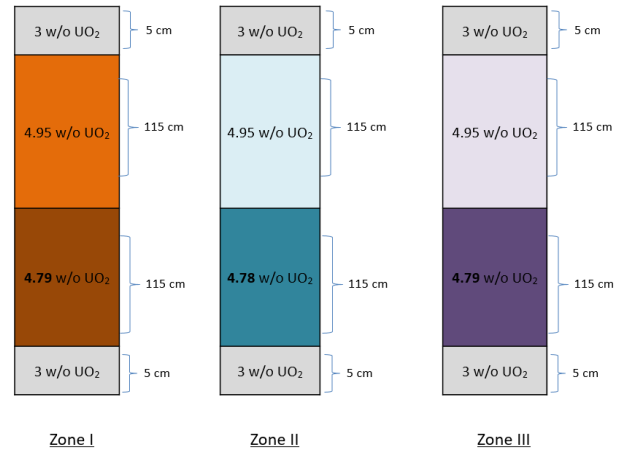
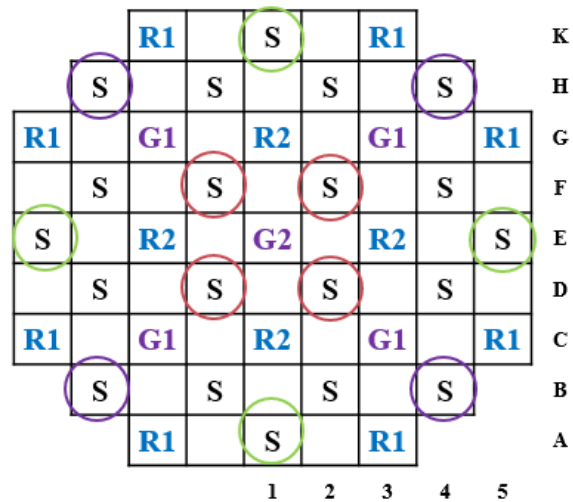


Figure 2. Axial fuel enrichment at each radial zone

## 2.4 Control Rod Specification

To attain the required shutdown margin without the utilization of soluble boron, it is imperative to raise the number of control element assemblies. Yet, over-indulging on this aspect could lead to the control rod driving mechanism failing to sustain the load. To this end, the core has opted for a checkerboard control rod pattern with extended fingers for the shutdown banks. There are two regulating banks for reactor startup from hot zero power and load-follow operations, and two gray banks for regulating reactivity during cycle and load-follow operations. Notably, the Gray bank G1 employs a heterogeneous material composition to improve the axial shape index (ASI) control during load-follow operations.



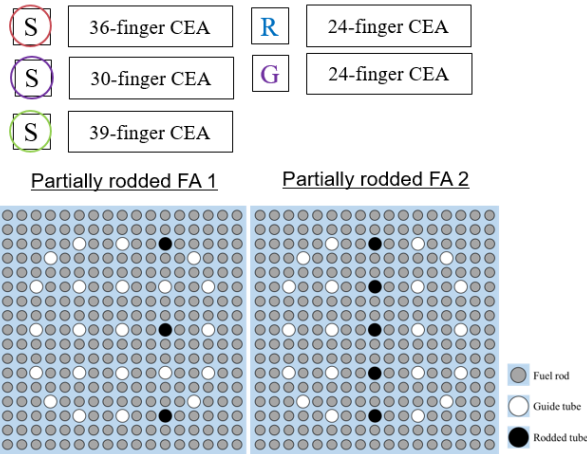


Figure 3. Bank positions (first) and checker-board pattern for shutdown banks (second)

Table 3. Composition and number of control rods

S	Shutdown Bank (90% B <sub>4</sub> C)	20
R2	Regulating Bank (Nat. B <sub>4</sub> C)	4
R1	Regulating Bank (50% B <sub>4</sub> C)	8
G2	SS-clad Mn	1
G1	160cm Inconel 625 (Upper) + 80cm Mn (Lower)	4
<b>Total</b>		<b>37</b>

### 3. Control Logic Mode-Y

In load-follow operations, the position of each bank is determined by a control logic referred to as Mode-Y. The insertion or withdrawal of a CEA is determined by the difference between core power and demand power, which is gauged by the difference in the coolant temperature. This temperature deviation measurement is both practical and conventional. If the temperature deviation falls outside of the predetermined dead-band, the logic adjusts the control rod until it returns to normal value. The second objective of the logic is to regulate the ASI value, even if the temperature deviation is still within the dead-band. It should be noted that high ASI is not always advantageous for core safety and economy.

Gray banks 1 and 2, as well as regulating bank 2 in the core can move independently to control the ASI value. In addition, they can move in opposite directions to regulate the ASI value simultaneously.

#### 3.1 Temperature and ASI Dead-band

In temperature dead-band, two ranges of dead-band are observed: slow and fast movements. Subject to deviation beyond the range, the rod should follow demand by moving faster. Specifically, the rod moves 10 times faster when the coolant temperature is out of the fast movement dead-band.

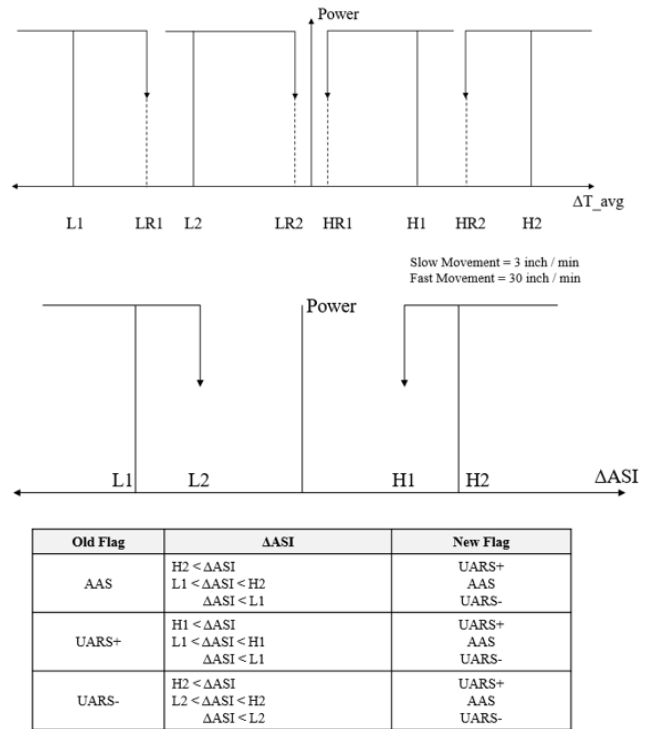


Figure 4. Temperature and ASI dead-band

#### 3.2 CEA Movement Logic

Table 4 displays the criteria for selecting the appropriate CEA based on power and ASI conditions. For power deviations, simple insertion or withdrawal will suffice. However, when ASI control is required, suitable CEAs are chosen, although their impact on the ASI reading may not always be favorable since power control is the primary goal.

Table 4. Bank movements for each power and ASI deviations

Direction	ASI Flag	CEA Position	Selected CEA	Effect
Insert	UARS+	G2 > B G2 = B, G1 > B G2 = B, G1 = B	G2 G1 R2	P If G2 < H/2 P If G1 < H/2 I
	UARS-	G2 > H/2 G2 < H/2, G1 > H/2 IF (G2 < H/2, G1 < H/2) THEN IF (R2 > H/2) THEN ELSE IF (G2 > B) THEN ELSE IF (G1 > B) THEN END IF END IF	G2 G1 R2 G2 G1	P P P N N
	AAS	G2 > B G2 = B, G1 > B G2 = B, G1 = B	G2 G1 R2	P If G2 < H/2 P If G1 < H/2 I

Direction	ASI Flag	CEA Position	Selected CEA	Effect
Withdraw	UARS+	R2 < UL	R2	P If R2 > H/2
		R2 = UL, G1 < UL	G1	P If G1 > H/2
		R2 = UL, G1 = UL	G2	P If G2 > H/2
	UARS-	R2 < UL	R2	P If R2 < H/2
		R2 = UL, G1 < H/2	G1	P
		R2 = UL, G1 = H/2, G2 < H/2	G2	P
AAS	R2 < UL	R2	P If R2 > H/2	
	R2 = UL, G1 < UL	G1	P If G1 > H/2	
	R2 = UL, G1 = UL	G2	P If G2 > H/2	
Direction	ASI Flag	CEA Position	Selected CEA	Effect
Normal	UARS+	IF (R2 > H/2, G1 < H/2)	R2 out, G1 in	P
		ELSEIF (G1 > H/2, G2 < H/2)	G1 out, G2 in	P
		ELSE	-	-
UARS-	UARS-	IF (R2 > H/2, G1 < H/2)	R2 in, G1 out	P
		ELSEIF (G1 > H/2, G2 < H/2)	G1 in, G2 out	P
		ELSE	-	-

#### 4. Numerical Results

To illustrate the load-follow operations, we utilize the in-house nodal solver KANT. The KANT code itself has been validated with various benchmarks [4]. The Monte Carlo code Serpent 2 produces the homogenized group constants and discontinuity factors. For this study, the neutronic solver is coupled with the thermal-hydraulic kernel for the analysis. In addition, the 2x2 NEM accelerated with CMFD is employed as the neutronic solver. The load-follow operations are replicated at three burnup points: the beginning of the cycle (BOC), the middle of the cycle (MOC) with 10 GWD/tU, and the end of the cycle (EOC) with 21 GWD/tU. The total transient duration is 72 hours, with 30 minutes required for a 50% increase or decrease in reactor power. The inlet temperature of the coolant was programmed with demand power and the steam generator was decoupled. During the transient simulations, the following parameters are calculated and plotted in the subsequent sub-sections: core power and demand power, bank position, ASI, and peaking factor. It is important to note that the local pin peaking factor of 1.1 is multiplied to 3D peaking factors as it represents a nodal value.

Overall, the core power closely tracks the demand power despite a rapid power change rate of 1.6% per minute. The independent banks G1, G2, and R2 use Mode-Y logic to regulate the reactor power and ASI values in the simulation.

##### 4.1 BOC

It is observed that the core power closely tracks the demand power while the ASI value is rather high around 0.23. Additionally, the peaking factor is still within the acceptable range.

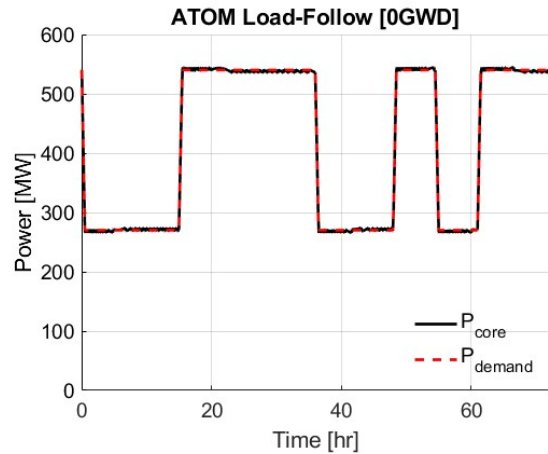


Figure 5. Core power and demand power at BOC

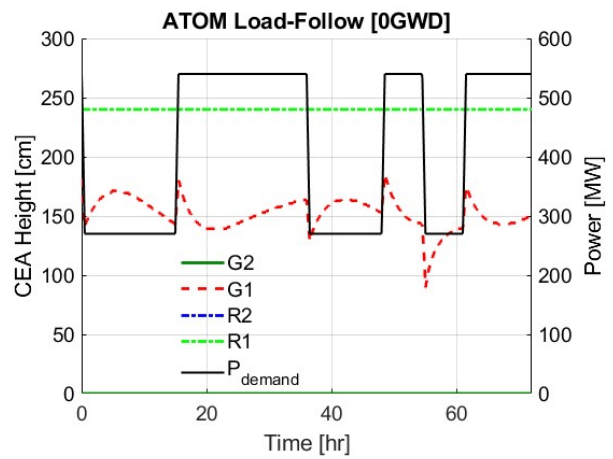


Figure 6. Bank position at BOC

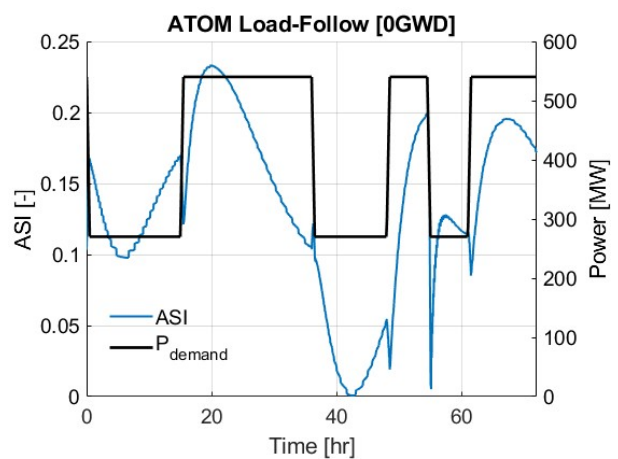


Figure 7. ASI value at BOC

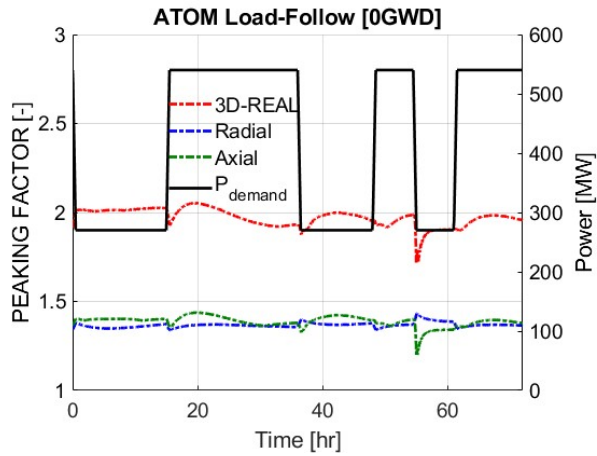


Figure 8. Peaking factors at BOC

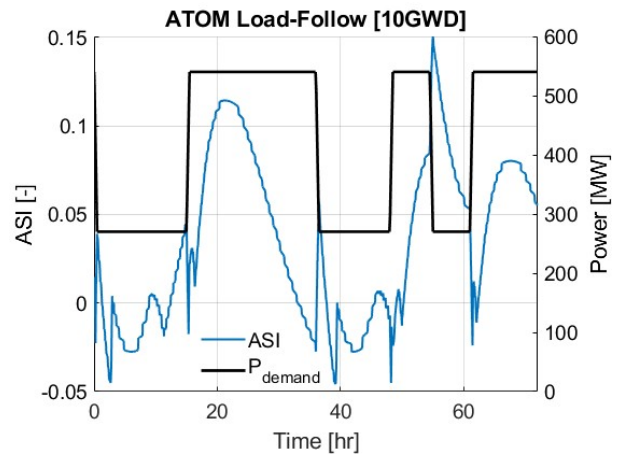


Figure 11. ASI value at MOC

#### 4.2 MOC

It is observed that the core power closely tracks the demand power while the ASI value is successfully controlled between -0.05 to 0.15. Additionally, the peaking factor is still within the acceptable range.

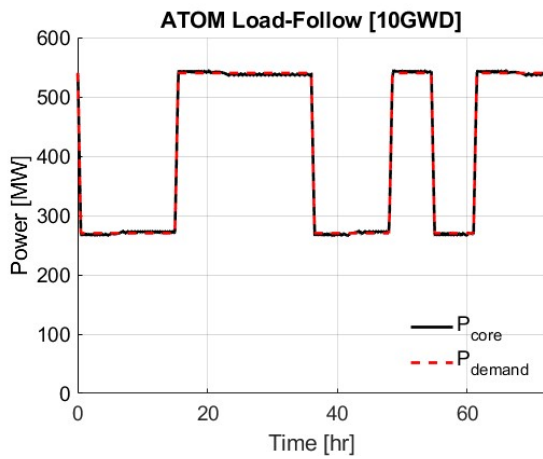


Figure 9. Core power and demand power at MOC

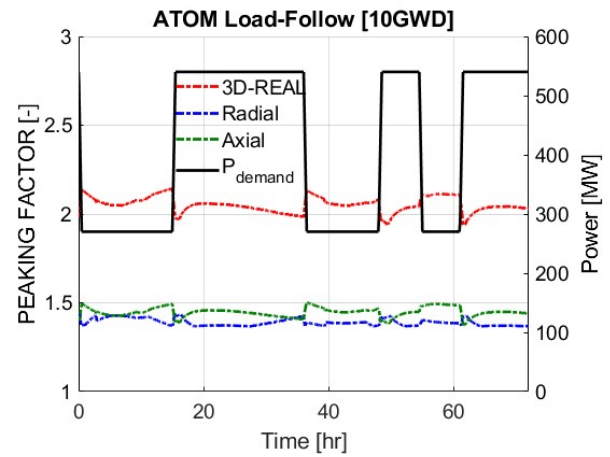


Figure 12. Peaking factors at MOC

#### 4.3 EOC

It is observed that the core power closely tracks the demand power while the ASI value is rather high around 0.24. Additionally, the peaking factor is still within the acceptable range.

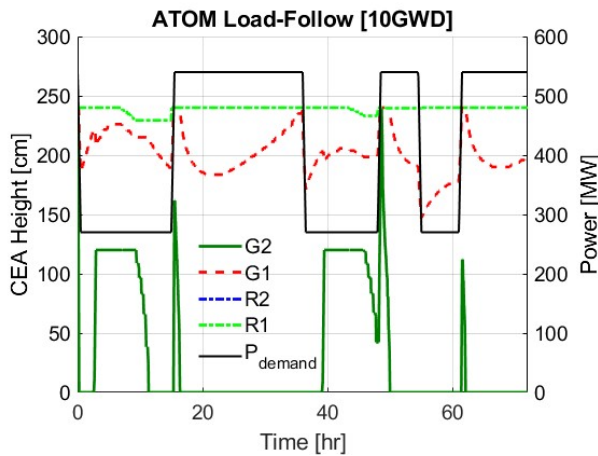


Figure 10. Bank position at MOC

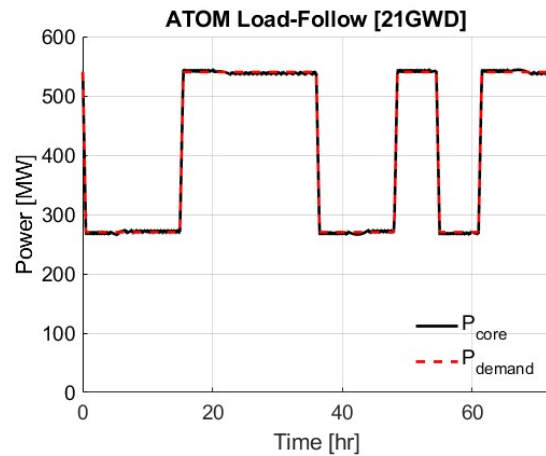


Figure 13. Core power and demand power at EOC

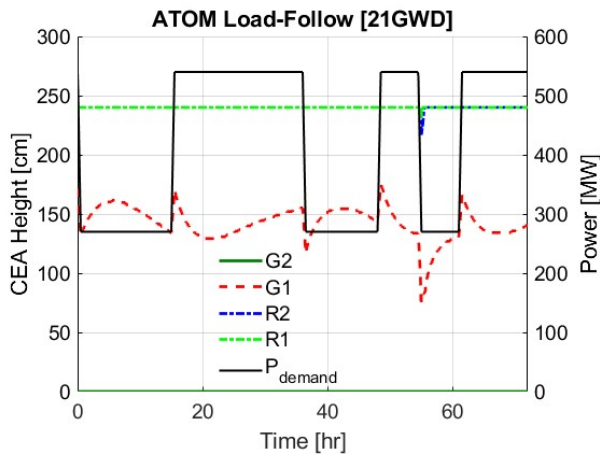


Figure 14. Bank position at EOC

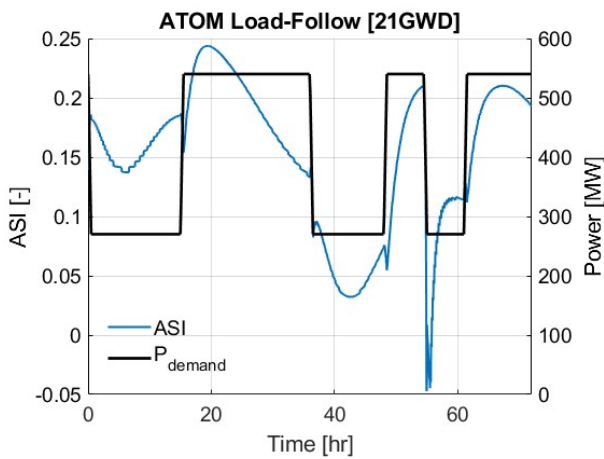


Figure 15. ASI value at EOC

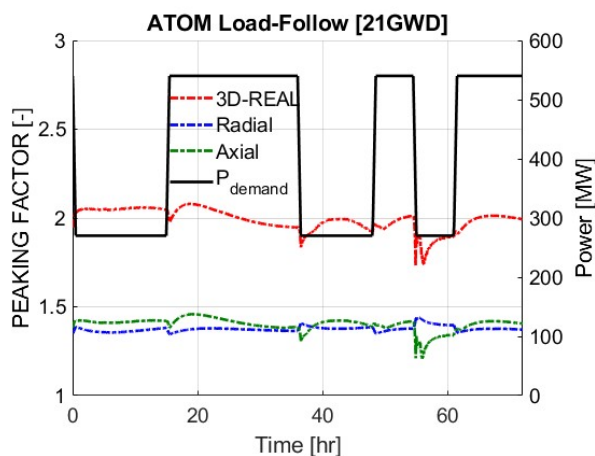


Figure 16. Peaking factors at EOC

## 5. Conclusions

In this study, we thoroughly investigated the power maneuvering capability of the ATOM core with control, employing the KANT code as the analytical tool. Of particular interest was the unique configuration of the ATOM core, with a power of 540 MW and active core height of 240 cm, which was studied over a range of burn-up conditions. Employing a consistent approach, whereby a programmed inlet coolant temperature is maintained to implement a constant average coolant temperature strategy, the control of the core is managed through the Mode-Y logic for the CEAs. It is noteworthy, throughout the 72-hour simulations, the core's power remained under effective control during the 72-hour simulations, even when dealing with relatively swift power changes. However, it should be noted at several conditions, such as BOC and EOC, the max ASI is  $\sim 0.23$  while the peaking factor is still within the acceptable range.

In future work, the hybrid CEA and the loading pattern will be re-optimized to reduce the Max ASI. Furthermore, we will revisit and re-optimize the Mode-Y logic to accommodate the hybrid CEA configuration. Additionally, the start-up scenario will be a focal point of investigation in our upcoming work.

## REFERENCES

- [1] OECD-NEA, "Technical and Economical Aspects of Load Following with Nuclear Power Plants," 2011.
- [2] Nguyen, Xuan Ha, ChiHyung Kim, and Yonghee Kim. "An advanced core design for a soluble-boron-free small modular reactor ATOM with centrally-shielded burnable absorber," *Nuclear Engineering and Technology* 51.2 (2019): 369-376.
- [3] Nguyen Xuan Ha, Seongdong Jang, and Yonghee Kim. "Truly-optimized PWR lattice for innovative soluble-boron-free small modular reactor," *Scientific reports* 11.1 (2021): 1-15
- [4] Taesuk Oh, et al., "Development and validation of multiphysics PWR core simulator KANT", Nuclear Engineering and Technology, In-press, 2023.